Sundus M. Ahmed[1], Nageeb S. Abtan[2], Ali H. Alwazir[3], Hakim S. Aljibori[3], Firas F. Sayyid[1], Ali M. Mustafa[1], Ahmed A. Alamiery[4,5], Abdul Amir H. Kadhum[6]

[1]Production Engineering and Metallurgy, University of Technology, Baghdad,Iraq, [2]Department of Mechanical Engineering, Tiktit University, College of Engineering, Tikreet, Salah Al Deen, Iraq, [3]College of Engineering, University of Warith Al-Anbiyaa, Karbalaa, Iraq, [4]I-Ayen Scientific Research Center, Al-Ayen Iraqi University, AUIQ, An Nasiriyah, Thi Qar, Iraq,[5]Department of Chemical and Process Engineering, Faculty of Engineering and Build Environment, Universiti Kebangsaan Malaysia, Bangi, Selangor, Malaysia, [6]Al-Ameed University College, Karbala, Iraq

Scientific paper
ISSN 0351-9465, E-ISSN 2466-2585
https://doi.org/10.62638/ZasMat1047

Zastita Materijala 66 ( )
(2025)

Investigation of FPM as a corrosion Inhibitor for mild steel in HCl solution: Insights from electrochemical, weight loss and theoretical approaches

ABSTRACT

In this study, we investigate the efficiency of furan-2-yl-piperazin-1-yl-methanone (FPM) as a corrosion inhibitor for mild steel in HCl environment. Our study combines electrochemical techniques, weight loss measurements and Density Functional Theory (DFT) calculations. Regarding weight loss experiments, we find that a concentration of 0.5 mM of FPM provides maximum protection efficacy, reaching 91.8% at 303 K after 30 minutes of immersion and observed that the inhibition efficiency rises with increasing concentration of FPM but declines with higher temperatures. Based on the Langmuir isotherm and experimental analysis, it can be suggested that FPM can adhere to the surface of mild steel through physical and chemical interactions. Moreover, our theoretical studies reveals correlations between the structure of FPM and its effectiveness in inhibiting corrosion, shedding light on the underlying mechanisms. Experimental and theoretical results both are in agreement. Our findings underscore the potential of FPM as a corrosion inhibitor in industrial applications, offering new avenues for corrosion control techniques.

Keywords: *Furan, corrosion, steel, potentiodynamic polarization, DFT*

1. INTRODUCTION

Corrosion is now a very difficult problem that is present in every industry. It has great and farreaching consequences in terms of both economics and safety. Not only are costs related to the direct degradation and replacement of materials incurred, but also the cost of other things that may include production losses, environmental damage, or simply safety compromised [1-3]. Mild steel certainly cuts across all these challenges as it can be totally relied upon. The attributes come with almost complete availability, good physical and chemical properties, and of course, affordability [4,5]. Hence, it forms the basis for almost all the industrial applications imaginable-from construction and infrastructure to different forms of manufacturing and the transport sector. Affordability and resilience are general characteristics that put mild steel into many different fields of engineering and different applications where it is needed for mechanical strength and ease of welding [6-9]. This notwithstanding, mild steel isknown to be corrosive especially in high-acid and moisture-laden environments. Effective corrosion control measures are effective in addressing the vulnerability. This emphasizes the continued research and innovation in discovering new corrosion inhibitors as well as protective coatings [10,11]. These strategies are capable of either saving valuable assets from damage or even improving the entire operational efficiency and health standards along with overall sustainability in the industries against corrosion damages to metallic structures and equipment [12-15]. In environments one encounters with hydrochloric acid (HCl)-containing gas, such as cleaning, pickling, metal etching, and chemical synthesis, corrosion in mild steel is found to be much more hazardous [16-18]. Among the special

Corresponding author: S.M.N. Ahmed
E-mail: dr.ahmed1975@gmail.com
Paper received: 26.10./2024
Paper corrected: 12.12.2024
Paper accepted: 15.12.2024

strategies investigated for corrosion mitigation agents are corrosion inhibitors. Such inhibitors are categorized based on their chemical form, mechanisms of internal action, and other relevant characteristics [19,20]. The copper-chromates and phosphate bases designed for purposes like corrosion inhibition have been the longtime backbone of any historic inorganic inhibitor [21-23]. But the problem of their environmental and health issue has led to investigations in other directions for organic inhibitors-their exactly current catching wave. Organic inhibitors are ornamented in a much more effective, multipurpose, and less harmful environmental and human impact. Compounds containing heteroatoms like nitrogen, oxygen, sulfur, and phosphorus show promising corrosion inhibition activity as these heteroatoms contribute to coordination bond formations where electrons from the heteroatoms are transferred to the free d-orbitals of iron atoms on the surface of mild steel. Corrosion inhibition ability decreases among these heteroatoms in the following order: oxygen (O), nitrogen (N), sulfur (S), and phosphorus (P) [24-27]. It is the electron density of the donor atom in the functional group of the inhibitor and polarizability of the functional group that affects the strength of chemisorption bond between the inhibitor molecules and the metal surface. Apart from these, electrostatic interactions between the inhibitor molecules and metal surface actually primarily accentuate the importance of such interactions with respect to corrosion inhibition mechanism [28,29].

Density Functional Theory (DFT), an extremely potent computation tool has already attracted great attention and created a strong demand for corrosion inhibition studies. DFT gives insights into the molecular structure, electronic properties, and adsorption behavior of inhibitor molecules that provide understanding of corrosion inhibition mechanisms at atomic levels [30-32]. This opens up FPM: furon-2-yl-piperazin-1-yl-methanone as a new interesting alternative for corrosion inhibition using its original structure combined with heteroatoms oxygen and nitrogen, as well as its heterocyclic rings. Those things together give an appropriate condition for favorable interactions with the metal surface to act in favor of the corrosion inhibition efficiency of FPM. This study aims to analyze the inhibition efficiency of this compound FPM (Figure 1) as an inhibitor of mild steel corrosion in 1N HCl solution. Through a holistic and synergistic collection of experimental techniques such as potentiodynamic polarization and theoretical methods like Density Functional Theory (DFT), we endeavor to explain the mechanism of corrosion inhibition by FPM. The whole originality of the research depends upon its comprehensive study, in which experimental and theoretical data will be combined to understand the corrosion inhibition potentiality of FPM in more nuanced detail. These studies aim primarily at understanding the inhibition characteristics of FPM, detailing its adsorption characteristics on mild steel surface, and correlating the experimental with the theoretical results. These studies will thus contribute to the advancement of corrosion control strategies applicable in achieving sustainable industrial practices and alleviating the harmful effects of corrosion on infrastructure and equipment.

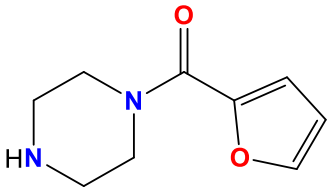

Figure 1. The chemical structure of FPM

2. METHODOLOGY

2.1. Materials

All chemicals utilized in this study were of reagent grade and procured from Sigma-Aldrich, Selangor, Malaysia. These chemicals were used without further purification. The purity of the compounds was confirmed through thin-layer chromatography (TLC) on silica gel G plates.

2.2. Electrochemical measurement

The experimental setup involved the preparation of mild steel samples, which were then immersed in hydrochloric acid (HCl) solution containing varying concentrations of FPM, the corrosion inhibitor under investigation. Potentiodynamic polarization measurements were conducted to evaluate the corrosion inhibition efficiency and to characterize the electrochemical behavior of the system. Mild steel specimens obtained from the Metal Samples Company were utilized as the working electrodes throughout the experimentation. The composition (wt%) of the mild steel was as follows: Fe, 99.21; C, 0.21; Si, 0.38; P, 0.09; S, 0.05; Al, 0.01. The specimens were cleaned in accordance with ASTM standard G1-03. The measurements were conducted in aerated, non-stirred 1.0 M HCl solutions at temperatures 303 K, with a FPM concentration range of 0.1–0.5 mM as the corrosion inhibitor [33-35]. Electrochemical measurements were performed using a Gamry water-jacketed glass cell containing three electrodes: the working, counter, and reference electrodes. These electrodes were composed of mild steel, a graphite bar, and a calomel electrode (SCE), respectively. A Gamry Instrument Potentiostat/Galvanostat/ZRA model Ref 600,

along with DC105 and EIS300 software by Gamry, was utilized for potentiodynamic scans. The potentiodynamic current-potential curves were swept from −0.25 to +0.25 VSCE at a scan rate of 0.5 mV•s^{-1}. Measurements were initiated approximately 30 minutes after immersing the working electrode in the solution to stabilize the steady-state potential. All measurements were conducted in triplicate, and average values were reported [36,37].

2.3. Weight-loss analysis

Weight-loss analysis involved immersing predetermined Mild Steel samples in 100 mL of HCl solution for 120 hours at an ambient temperature of 303 K. After every 24-hour interval, the samples were withdrawn from the acid solution, rinsed thoroughly with distilled water and acetone, dried, and re-weighed following ASTM G31-12a guidelines. Corrosion rate (C_R mm/y) and percentage inhibition efficiency (IE%) were computed based on the weight loss data collected during the exposure period [33-35]. The corrosion rate (CR) was calculated using Eq. (1)

$$C_R = \frac{87.6W}{dat} \quad (1)$$

Where W represents the weight loss in milligrams, d is the density in grams per cubic centimeter, a denotes the total area in square centimeters, t signifies the exposure time in hours, the constant 87.6 is included in the formula.

Percentage inhibition efficiency (IE) was determined using the Eq. (2):

$$IE = \frac{w_1 - w_2}{w_1} \times 100 \quad (2)$$

w_1 and w_2 represent the weight loss of specimens in the presence and absence of specific concentrations of FPM, respectively.

The inhibition efficiency was calculated for each FPM concentration throughout the exposure duration. Surface coverage (θ) was evaluated using the equation:

$$\theta = \frac{w_1 - w_2}{w_1} \quad (3)$$

Where θ denotes the quantitative amount of FPM compound adsorbed per gram on the steel specimens.

2.4. Computational Studies

The theoretical component of this study employed Density Functional Theory (DFT) calculations to investigate the molecular structure, electronic properties, and adsorption behavior of FPM on the mild steel surface. DFT simulations provided insights into the interaction mechanisms between FPM molecules and the metal surface, elucidating the underlying principles of corrosion inhibition [38,39]. Quantum chemical computations were performed using ChemOffice software. Becke's three-parameter hybrid functional (B3LYP) level within Gaussian 03 version, with 6–31G as the reference set, was utilized to investigate the chemical reactivity of the FPM molecule. Quantum parameters such as energy gap (ΔE), fraction of electron transfer (ΔN), dipole moment (μ), ionization energy (I), electron affinity (A), absolute electronegativity (χ), hardness (η), and softness (σ) were determined for FPM in the gas phase [40].

The quantum chemical parameters, including χ, η, σ, and ΔN, were calculated using Equations (4)–(9) [41]:

$$I = -E_{HOMO} \quad (4)$$

$$A = -E_{LUMO} \quad (5)$$

$$\chi = (I + A)/2 \quad (6)$$

$$\eta = (I - A)/2 \quad (7)$$

$$\sigma = 1/\eta \quad (8)$$

$$\Delta N = (\chi_{Fe} - \chi_{inh})/2(\eta_{Fe} - \eta_{inh}) \quad (9)$$

3. RESULTS AND DISCUSSION

3.1. Potentiodynamic Polarization Analysis

As a result, the most valuable results of the potentiodynamic polarization tests are those on the efficiency achieved by different concentrations and immersions of Furan-2-yl-piperazin-1-yl-methanone (FPM) in terms of inhibiting corrosion. Deriving these tests also made it possible to determine other precious electrochemical parameters such as corrosion potential, corrosion current density, and polarization resistance. In addition, surface analysis techniques provided visual evidence of the protective film formed on the mild steel surface in the presence of FPM. They are associated with the anodic and cathodic polarization behavior, showing the electrochemical effect of FPM on mild steel corrosion in 1 M HCl acid solution, as pictorially shown in Figure 2. Table 1 presents the outcomes derived from the polarization scans [42]. Notably, the corrosion rates displayed in Table 1 demonstrate a substantial difference between FPM inhibited and uninhibited mild steel samples. At 0.0 mM FPM concentration, significant anodic dissolution of the mild steel sample occurred, accompanied by the formation of pores, pits, and channels within the porous oxide layer [43,44]. This corrosion was primarily instigated by Cl− ions present in the acid solution, facilitating corrosion reactions on the steel surface. A remarkable decrease in corrosion rate was observed as FPM concentration increased from 0.1 to 0.5 mM. This reduction can be attributed to the complex and

non-homogeneous nature of metallic corrosion, characterized by numerous anodic and cathodic reaction cells. Corrosion inhibiting compounds such as FPM tend to interact with these cells, either by retarding the redox electrochemical process or inhibiting the diffusion of active corrosive anions from the acid solution to the mild steel surface. Furthermore, variations in FPM concentration significantly impacted the inhibition efficiency values. It was observed that FPM's inhibition performance is dependent on its concentration. For instance, at 0.5 mM FPM concentration, the inhibition efficiency reached 90.7%, while at 0.1 mM FPM, the inhibition efficiency was 65.3%. The potentiodynamic polarization parameters calculated from Tafel curves for mild steel in both uninhibited and inhibited acidic solutions at 303 K are summarized in Table 1. These parameters provide quantitative data regarding the electrochemical behavior of mild steel in the presence of FPM, further elucidating its corrosion inhibition mechanism [45,46].

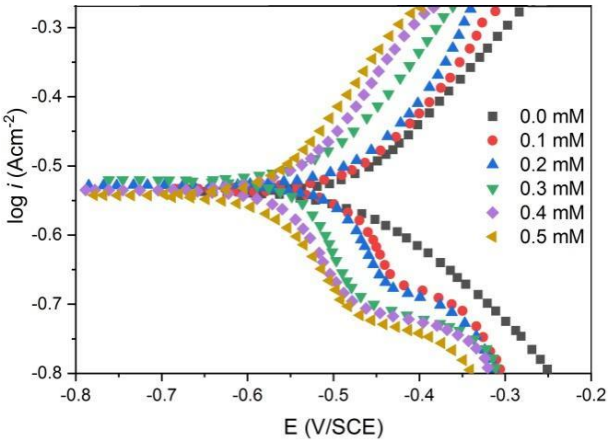

Figure 2. Potentiodynamic Polarization curves of the mild steel in the uninhibited and inhibited corrosive solution of various inhibitor concentrations.

Table 1. Potentiodynamic Polarization Parameters for Mild Steel in Acidic Solution, with and without Inhibition, at 303 K

Conc.	−Ecorr (V vs. SCE)	−βc (mV dec−1)	icorr (μAcm−2)	IE(%)
0.0	503	147	602	0
0.1	492	196	62.7	65.3
0.2	495	180	89.3	73.5
0.3	497	168	121.5	80.1
0.4	507	150	142.6	84.6
0.5	510	143	175.7	90.7

3.2. Weight loss measurements

3.2.1. Effect of Inhibitor Concentrations

Figure 3 provides insights into the influence of inhibitor concentrations on the corrosion behavior of mild steel during a 24-hour immersion period at 303 K. It is evident that increasing the concentration of the inhibitor (FPM) from 0.0 mM to 0.5 mM leads to a significant reduction in the corrosion rate. For instance, at 0.0 mM inhibitor concentration, the corrosion rate is recorded at 1.294 mg/cm²·h. However, with increasing inhibitor concentrations, the corrosion rate steadily decreases. At 0.5 mM inhibitor concentration, the corrosion rate reaches its lowest value of 0.121 mg/cm²·h, representing an impressive reduction in corrosion rate compared to the uninhibited sample [47]. This observed decrease in corrosion rate with increasing inhibitor concentration highlights the effectiveness of FPM in mitigating corrosion of mild steel. As the concentration of FPM increases, more inhibitor molecules are available to form a protective barrier on the metal surface, thereby hindering corrosive processes. Furthermore, the inhibition efficiency exhibits a corresponding increase with rising inhibitor concentrations [48]. At 0.1 mM inhibitor concentration, the inhibition efficiency is measured at 54.9%, which steadily increases to 91.7% at 0.5 mM inhibitor concentration. The significant enhancement in inhibition efficiency with increasing inhibitor concentration underscores the potent corrosion inhibition properties of FPM. Higher inhibitor concentrations result in greater coverage of the metal surface by inhibitor molecules, leading to more effective corrosion protection.

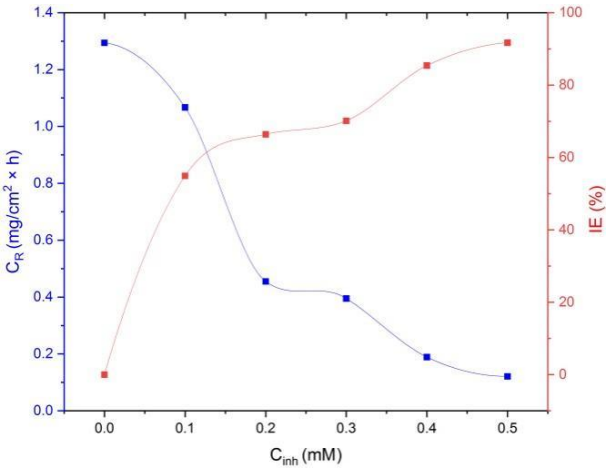

Figure 3. Effect of inhibitor concentrations for 24 hours as immersion time and 303 K

Overall, the data presented in Figure 3 demonstrate the strong correlation between inhibitor concentration, corrosion rate reduction, and inhibition efficiency improvement. These findings underscore the potential of FPM as a highly effective corrosion inhibitor for mild steel, particularly at elevated concentrations [49,50].

3.2.2. Effect of Temperature

The influence of temperature and concentrations of inhibitors on the inhibition of mild steel corrosion is presented in figure 4. Inhibition efficiency decreases with increased temperature. Increasing temperature curbs inhibition efficiency, which states that it is difficult to control corrosion at higher temperatures. Penetrating cause corrosion rates steadily increases and increases temperature for inhibition efficiency because several situations are involved [51,52]. The first is that high temperature accelerates the kinetics of reactions such that they have greater rates of dissolution for metals. Higher temperature may affect adsorption of inhibitor molecules on the metal surface, thus making their efficiency in forming protective barriers against diffusing corrosive agents less effective. Data reaction, therefore, gives an insight into how temperature is critical in determining the corrosion behavior of mild steel in the presence of inhibitors. Temperatures, therefore, should be considered when developing strategies or putting together a protocol for their use in corrosion control. This is particularly true for application at high temperatures, as they offer a likelihood of increasing corrosion rates [53,54].

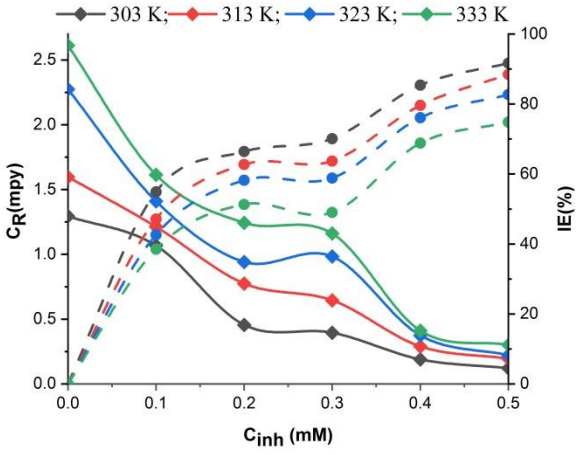

Figure 4. Impact of Temperature and Inhibitor Concentrations on Corrosion Rate and Inhibition Efficiency of Mild Steel Samples Immersed in 1 M HCl Solution for 24 Hours

3.2.3. Effect of Duration Periods

The evolution of immersion time and inhibitor concentrations on the corrosion behavior of mild steel is represented by Figure 5. It indicates that with increase in the immersion period, there is a significant increase in corrosion rate at all inhibitor concentrations [55]. Furthermore, it was also found that at all immersion periods as the concentration of inhibitor increases, the corrosion attack decreases. The trend continues throughout different immersion periods showing that higher concentrations of inhibitors are better for corrosion control. Over time as the immersion period increases, there is a gradual decrease in inhibition efficiency for all concentrations of inhibitors [56]. Inhibition efficiency decreases as immersion time increases suggesting that the protective barrier created by the inhibitor molecules on the metal surface weaken with prolonged exposure [57]. The increase in corrosion rate with immersion time and decrease in inhibition efficiency with immersion time is due to the slow degradation and depletion of the inhibitor molecules from the surface of the metal. As time of immersion increases, the inhibitor molecules lose their activity due to desorption or chemical degradation which leads to low corrosion prevention. Overall, the data in Figure 5 speaks of how dynamic the corrosion processes are and how the rates and effectiveness of inhibition are impacted by concentrations of the inhibitors and immersion durations. This information presents approaches to the development of corrosion control methodologies with consideration for the continuous monitoring and optimization aspects of concentration and immersion durations in effective corrosion control practices for extended times [58].

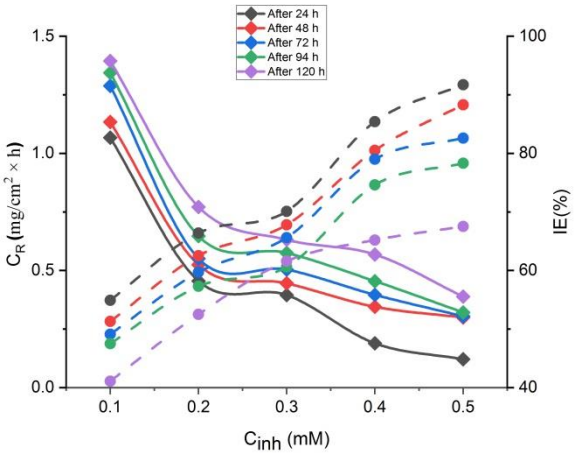

Figure 5. Impact of Immersion Periods and FPM Concentrations on C_R and IE% of Mild Steel Samples Immersed in 1 M HCl at 303 K

3.3. Adsorption Isotherm

The formation of a protective layer on the electrode surface, denoted as θ, is intimately linked with the adsorption phenomenon. Various

adsorption isotherm models, including Temkin, Frumkin, Flory-Huggins, and Langmuir, have been employed to analyze weight loss data by establishing the relationship between inhibitor concentration (C_{inh}) and surface coverage (θ) [59]. Among these models, the Langmuir adsorption isotherm demonstrated superior fitting capability, characterized by a high correlation coefficient (R^2), as depicted in Figure 6. This model effectively describes the inhibitor adsorption process through Equation 10 [60]:

$$\frac{C}{\theta} = \frac{1}{K_{ads}} + C \qquad (10)$$

Here, θ represents the surface coverage, K_{ads} denotes the adsorption constant, and C signifies the inhibitor concentration. To further elucidate the inhibitor adsorption process, the adsorption free energy (ΔG^0_{ads}) was calculated utilizing the K_{ads} value with Equation 11:

$$\Delta G^0_{ads} = \frac{1}{55.5} exp(-K_{ads}/RT) \qquad (11)$$

In this equation, the molar concentration of water (55.5 M) and the gas constant (R) under standard conditions are considered. This calculation provides valuable insights into the thermodynamic aspects of inhibitor adsorption, aiding in the comprehensive understanding of the corrosion inhibition mechanism.

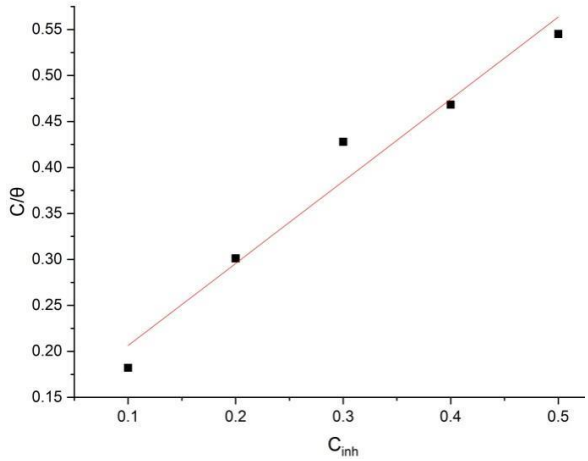

Figure 6. Langmuir isotherm adsorption of FPM on the mild steel surface in 1 M HCl at 303 K from the weight loss analysis

The Langmuir isotherm parameters throw light on the adsorption behaviour of the inhibitor molecules on the mild steel surface in 1 M HCl at 303 K. The Langmuir isotherm parameters derived from the weight loss analysis are shown in Table 2. By Langmuir adsorption constant (K_{ads}) we mean the strength of inhibitor adsorption on the metal surface. Higher value of K_{ads} means stronger adsorption of inhibitor molecules onto the mild steel surface. In this case, the calculated K_{ads} value of 11.20×10^5 L/mg indicates that adsorption strength is quite significant and inhibition is very effective [61].

Table 2. Langmuir Isotherm Parameters: Adsorption of Tested Inhibitor Molecules on the Mild Steel Surface in 1 M HCl at 303 K from Weight Loss Analysis.

Parameter	Weight loss
Intercept	0.116
R^2	0.96569
slope	0.893
K	11.20 (L/mg) × 10^5
ΔG	-40.75 kJ/mol

Moreover, the adsorption free energy, denoted as (ΔG^0_{ads}) eveals the spontaneity of the adsorption process. A negative value of ΔG^0_{ads} points towards the spontaneous nature of the adsorption process, which indicates that the inhibitor molecules are favorably adsorbed on the mild steel surface. The observed value of -40.75 kJ/mol under ΔG^0_{ads} proves that the adsorption process is highly spontaneous further reaffirming the competence of the inhibitor in curbing corrosion [62].

The high value of ΔG^0_{ads} shows that the inhibitor molecules are strongly chemically adsorbed by the acid. The electrons are moved from the high electron centers to the empty 3d orbital of iron (Fe) to form a covalent bond between the metal surface and the inhibitor molecules. Such covalent bond formation strengthens the protective layer over the mild steel surface, which effectively inhibits the corrosion rate. It can be summarized that the parameters of the Langmuir isotherm show that these inhibitors tested can be adsorbed strongly and they spontaneously adsorb onto the mild steel surface, demonstrating their efficiency in corrosion inhibition. These findings show that the inhibitor molecules definitely have high potential for practical applications in corrosion control approaches.

3.4. DFT Analysis

This is revealed through frontier molecular orbital theory (FMOT) coupled with Density Functional Theory (DFT) software, which explains the adsorption ability of their molecules in their associated mild steel surfaces. The quantum chemical parameters summarized in Table 3 will serve as significant insight into the efforts to extricate the relationship between molecular properties and inhibition efficiency of Furan-2-yl-piperazin-1-yl-methanone (FPM) as a corrosion inhibitor. The HOMO and LUMO energies are

indicative of the electron donation and acceptance abilities of the molecule FPM, respectively [63,64]. Here, the HOMO energy of FPM is fairly low at -10.026eV indicating a strong tendency to donate electrons, while the LUMO energy is 0.463eV which suggests it can accept electrons. Absolute electron negativity values (measured as χ) and hardness (η) further characterized by FPM's intrinsic quality with calculated values. A low value of χ (-4.282eV) indicates FPM is a very strong electron Lovelock, while a high hardness value (-5.244eV) suggests FPM's resistance to any variations in density of electrons. Moreover, the softness (σ) parameter, calculated to be -0.190 eV^{-1}, signifies FPM's propensity for electron donation or acceptance. A higher value of σ indicates greater reactivity of the molecule. The dipole moment (μ) and Fraction of Electron Transfer (ΔN) provide additional insights into FPM's interaction with the metal surface. The negative dipole moment (-5.14) suggests a nonuniform charge distribution over the molecule, facilitating its adsorption onto the metal surface. Furthermore, the negative ΔN value (-0.2114) indicates electron transfer from FPM to the metal surface, which correlates with enhanced inhibition efficiency [65,66]. In accordance with Lukovit's study, inhibition performance correlates positively with the fraction of electron transfer (ΔN), with optimal inhibition observed when ΔN is less than 3.6 [67].

Table 3. Quantum Chemical Parameters for FPM as a Corrosion Inhibitor

HOMO (eV)	LUMO (eV)	χ (eV)	η (eV)	σ (eV^{-1})	μ	ΔN
-10.026	0.463	-4.282	-5.244	-0.190	-5.14	-0.2114

Based on Figure 7, the distribution of HOMO electron density is predominantly observed over the aromatic benzene ring and the carbonyl group of the inhibitor molecule. This spatial distribution indicates potential sites for interaction between the inhibitor and the metal surface. When the inhibitor molecule adsorbs onto the metal surface, it is likely that charge donation from the inhibitor molecules to the vacant d-orbitals of the iron atoms will occur. This charge transfer process is crucial for forming a protective layer on the metal surface, thereby inhibiting corrosion. The interaction between the HOMO of the inhibitor and the metal surface promotes the formation of stable bonds, contributing to the inhibition efficiency [68,69].

The electron density in LUMO is spread over the inhibitor molecule. This indicates that possible back-donation from the occupied orbitals of the metal to the inhibitor will involve various regions of the inhibitor molecule for interaction. This is essential to getting the inhibitor molecule adsorbed on the metal substrate. The back-donation process, it may be noted, is necessary for stabilizing the adsorbed inhibitor molecule on the metal surface. By getting electrons back from the metal surface, it can hold itself really well and inhibit the corrosion. The wider distribution of electron density in the LUMO suggests that it is indeed versatile in that respect; it contributes to the overall effectiveness of corrosion inhibition as well in interaction of that inhibitor molecule under metal surface. Hence, it can be inferred that the electron density distribution on both these HOMO and LUMO orbitals is of paramount importance concerning the interaction between the inhibitor molecule and the metal surface. All of these include charge transfer processes, which are necessary to produce a protective layer and inhibit the corrosion [70].

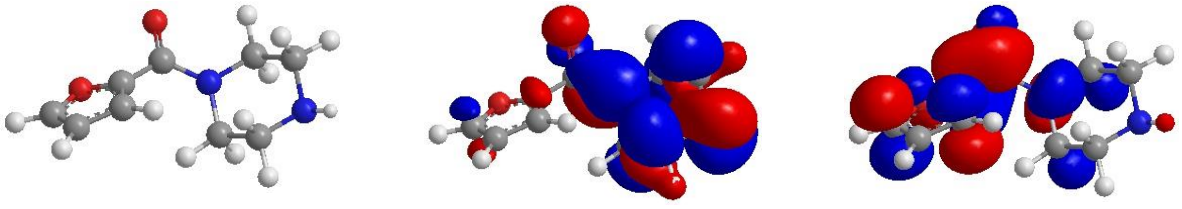

a b c

Figure 7. Various aspects of the tested inhibitor: (a) the optimized structure, (b) the highest occupied molecular orbitals (HOMO), and (c) the lowest unoccupied molecular orbitals (LUMO)

In considering the effects of atomic charges on the inhibition of corrosion, Figure 8 offers valuable insights'. The data indicate that the negative charges on oxygen atoms O8 and O9 are -0.85 eV and -0.28 eV, respectively. Similarly, nitrogen atoms N3 and N6 carry negative charges of -0.66 eV and -0.2 eV, respectively. The above values suggest that there is a surplus of electrons around these atoms, making these regions electron-rich within the inhibitor molecule. These electron-rich regions further indicate that they play a vital role in corrosion inhibition by facilitating the interaction

between the metal surface with the molecule. Oxygen and nitrogen, particularly, have a high affinity for positively charged metal ions at the surface [71,72]. By forming coordination bonds with these metal ions, the inhibitor molecules can adsorb onto the metal surface, thereby forming a protective barrier against corrosive agents. Having negatively charged surfaces further enhances electron donation to the substrate. This process of electron donation works towards stabilizing the adsorbed inhibitor molecules as they promote passive film formation, inhibiting corrosion. Overall, it is significantly useful against corrosion in that negative atomic charges on the oxygen and nitrogen atoms of the inhibitor molecule contribute towards their different functions in corrosion inhibition. These functions include facilitating adsorption and electron transfer processes at the metal surface, which further improve the corrosion effectiveness of the inhibitor [73].

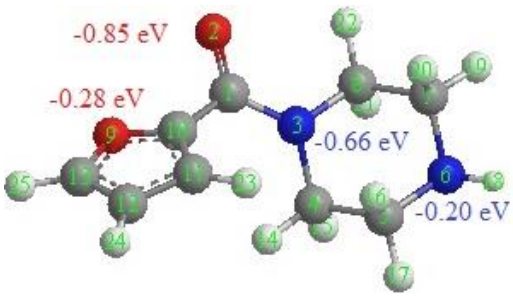

Figure 8. The atomic charges of tested inhibitor molecule

3.5. Mechanism of inhibition action

FPM inhibition mechanism on mild steel in HCl showed in figure 9. The elucidation of the adsorption mechanism of the inhibitor is vital to understand its inhibitive action, whether ionic or molecular. The major modes of adsorption can depend mainly on the nature of the chemical species of the inhibitor and the type of acid anion present. FPM contains chemical components such as carbonyl groups, double bonds, as well as oxygen and nitrogen heteroatoms, aligning with the general characteristics of corrosion inhibitors. Chloride ions are known for their high absorptivity, suggesting their potential impact on inhibitor adherence, particularly in halide-containing solutions. Thermodynamic and kinetic parameters obtained from the study indicate the physical adsorption of FPM on the mild steel surface in acidic solutions. The increased efficacy of the inhibitor, as evidenced by weight loss measurements, suggests more efficient adsorption on the mild steel substrate, effectively covering the surface-active sites and thereby significantly reducing the corrosion rate. In acidic solutions, FPM likely undergoes protonation, leading to a positive surface charge on the corroded mild steel surface, which may affect its adsorption behavior. Initially, adsorption of chloride acid anions occurs, introducing additional negative charges to the solution, thereby facilitating the adsorption of cations. Subsequently, through van der Waals interactions, the protonated inhibitor accumulates on the negatively charged metal surface, forming coordinate bonds by partially transferring electrons from the nitrogen and oxygen heteroatoms and multiple bonds to the unfilled d-orbitals of iron. FPM may also interact with Fe^2+ ions formed on the steel surface due to the presence of unshared electron pairs on nitrogen and oxygen atoms, forming metal-inhibitor complexes. These complexes adhere to the steel surface through van der Waals forces, creating a protective layer that effectively inhibits corrosion. In summary, the inhibition mechanism of FPM involves its adsorption on the mild steel surface through a combination of ionic and molecular interactions, forming protective complexes that prevent corrosion.

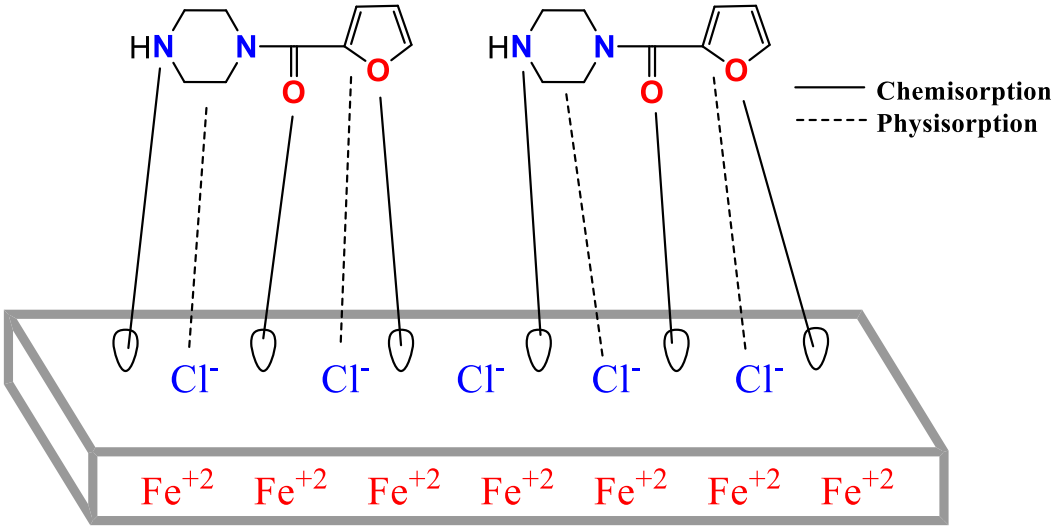

Figure 9. Schematic illustrative diagram of corrosion inhibition mechanism of FPMin acid solution

4. CONCLUSION

The study was aimed at determining the corrosion inhibition efficiency of furan-2-yl-piperazin-1-yl-methanone (FPM) for low carbon steel in hydrochloric acid (HCl) solution. Both experimental and theoretical techniques contributed significantly to understanding FPM's corrosion inhibition mechanism. Experimental results also reaffirmed that FPM is quite an efficient inhibitor, the most protection efficiency being 91.8% at 303 K after holding the specimen for 30 minutes. The increase in FPM concentration improved the inhibition efficiency, but it decreased as the temperature increased, indicating that both factors played roles in the inhibition effectiveness. From the prediction, FPM may be adsorbed on the mild steel surface through physical and chemical bonds, following the Langmuir adsorption isotherm model. Theoretical investigations using Density Functional Theory (DFT) have shown a better understanding of the molecular structure of FPM and its relationship with the experimental inhibition efficiency. The adsorption ability of FPM as deduced by quantum chemical parameters like HOMO and LUMO energy values implied proper interaction with the mild steel surface and contributed to its action against corrosion [74]. Overall, the complete combination of experimental and theoretical methods hold bright future prospects for the application of FPM as a corrosion inhibitor in industrial settings. FPM will definitely help realize the much needed improvements in corrosion control strategies for attaining durable and safe as well as sustainable industrial applications by providing mild steel with effective protection against corrosion.

5. REFERENCES

[1] N.S. Abtan, M.A.I. Al-Hamid, L.A. Kadhim, F.A. Sayyid, F.T.M. Noori, A. Kadum, A. Alamiery, W.K. Al-Azzawi (2024) Unlocking the Power of 4-Acetamidoantipyrine: A Promising Corrosion Inhibitor for Preserving Mild Steel in Harsh Hydrochloric Acid Environments. Prog. Color Colorants Coat., 17(1), 85–96, https://doi.org/10.30509/pccc.2023.167147.1223.

[2] A.N. Jasim, A. Mohammed, A.M. Mustafa, F.F. Sayyid, H.S. Aljibori, W.K. Al-Azzawi, A.A. Al-Amiery, E.A. Yousif (2024) Corrosion Inhibition of Mild Steel in HCl Solution by 2-acetylpyrazine: Weight Loss and DFT Studies on Immersion Time and Temperature Effects. Prog. Color Colorants Coat., 17(4), 333–350, https://doi.org/10.30509/pccc.2024.167231.1261.

[3] A.F. Hamood, H.S. Aljibori, M.A.I. Al-Hamid, A.A. Alamiery, W.K. Al-Azzawi (2024) MOP as a Corrosion Inhibitor for Mild Steel in HCl Solution: A Comprehensive Study. Prog. Color Colorants Coat., 17(3), 207–226, https://doi.org/10.30509/pccc.2023.167176.1237.

[4] M.M. Taha, S.A. Nawi, A.M. Mustafa, F.F. Sayyid, M.M. Hanoon, A.A. Al-Amiery, A.A.H. Kadhum, W.K. Al-Azzawi (2024) Revolutionizing Corrosion Defense: Unlocking the Power of Expired BCAA. Prog. Color Colorants Coat., 17(2), 97–111, https://doi.org/10.30509/pccc.2023.167156.1228.

[5] A.M. Resen, A.N. Jasim, H.S. Qasim, M.M. Hanoon, A.A. Al-Amiery, W.K. Al-Azzawi, A.M. Mustafa, F.F. Sayyid (2024) Investigating the Corrosion Inhibition Performance of Methyl 3H-2,3,5-triazole-1-formate for Mild Steel in Hydrochloric Acid Solution: Experimental and Theoretical Insights. Prog. Color Colorants Coat., 17(2), 185–205, https://doi.org/10.30509/pccc.2023.167189.1245.

[6] M.K. Abbass, K.M. Raheef, I.A. Aziz, M.M. Hanoon, A.M. Mustafa, W.K. Al-Azzawi, A.A. Al-Amiery, A.A.H. Kadhum (2024) Evaluation of 2-Dimethylaminopropionamidoantipyrine as a Corrosion Inhibitor for Mild Steel in HCl Solution: A Combined Experimental and Theoretical Study. Prog. Color Colorants Coat., 17(1), 1–10, https://doi.org/10.30509/pccc.2023.167081.1197.

[7] H.S. Aljibori, O.H. Abdulzahra, A.J. Al-Adily, W.K. Al-Azzawi, A. Al-Amiery, A.A.H. Kadhum (2023) Corrosion inhibition effects of concentration of 2-oxo-3-hydrazonoindoline in acidic solution, exposure period, and temperature. Int. J. Corr. Scale Inhib., 12(2), 438–457, https://doi.org/10.17675/2305-6894-2023-12-2-4.

[8] S. Junaedi, A.A.H. Kadhum, A. Al-Amiery, A.B. Mohamad, M.S. Takriff (2012) Synthesis and characterization of novel corrosion inhibitor derived from oleic acid: 2-Amino-5-Oleyl 1,3,4-Thiadiazol (AOT). Int. J. Electrochem. Sci., 7(4), 3543–3554.

[9] H.S. Aljibori, A.H. Alwazir, S. Abdulhadi, W.K. Al-Azzawi, A.A.H. Kadhum, L.M. Shaker, A.A. Al-Amiery, H.Sh. Majdi (2022) The use of a Schiff base derivative to inhibit mild steel corrosion in 1 M HCl solution: a comparison of practical and theoretical findings. Int. J. Corr. Scale Inhib., 11(2), 1435–1455.

[10] W.K. Al-Azzawi, S.M. Salih, A. Hamood, R.K. Al-Azzawi, M.H. Kzar, H.N. Jawoosh, L.M. Shakier, A. Al-Amiery, A.A.H. Kadhum, W.N.R.W. Isahak, M.S. Takriff (2022) Adsorption and theoretical investigations of a Schiff base for corrosion inhibition of mild steel in an acidic environment. Int. J. Corr. Scale Inhib., 11(2), 1063–1082.

[11] D.M. Jamil, A. Al-Okbi, M. Hanon, K.S. Rida, A. Alkaim, A. Al-Amiery, A. Kadhum, A.A.H. Kadhum (2018) Carbethoxythiazole corrosion inhibitor: as an experimentally model and DFT theory. J. Eng. Appl. Sci., 13(11), 3952–3959.

[12] A. Alobaidy, A. Kadhum, S. Al-Baghdadi, A. Al-Amiery, A. Kadhum, E. Yousif, A.B. Mohamad (2015) Eco-friendly corrosion inhibitor: experimental studies on the corrosion inhibition performance of creatinine for mild steel in HCl complemented with quantum chemical calculations. Int. J. Electrochem. Sci., 10(3), 3961–3972.

[13] A.A. Alamiery (2022) Study of corrosion behavior of N'-(2-(2-oxomethylpyrrol-1-yl)ethyl)piperidine for mild steel in the acid environment. Biointerface Res. Appl. Chem., 12(3), 3638–3646.

[14] A. Alamiery, A.B. Mohamad, A.A.H. Kadhum, M.S. Takriff (2022) Comparative data on corrosion protection of mild steel in HCl using two new thiazoles. Data Brief, 40, 107838, https://doi.org/10.1016/j.dib.2022.107838.

[15] A.M. Mustafa, F.F. Sayyid, N. Betti, L.M. Shaker, M.M. Hanoon, A.A. Alamiery, A.A.H. Kadhum, M.S. Takriff (2022) Inhibition of mild steel corrosion in hydrochloric acid environment by 1-amino-2-mercapto-5-(4-(pyrrol-1-yl)phenyl)-1,3,4-triazole. S. Afr. J. Chem. Eng., 39(4), 42–51, https://doi.org/10.1016/j.sajce.2021.11.009.

[16] A.A. Alamiery (2022) Investigations on corrosion inhibitory effect of newly quinoline derivative on mild steel in HCl solution complemented with antibacterial studies. Biointerface Res. Appl. Chem., 12(4), 1561–1568.

[17] I.A.A. Aziz, I.A. Annon, M.H. Abdulkareem, M.M. Hanoon, M.H. Alkaabi, L.M. Shaker, A.A. Alamiery, W.N.R.W. Isahak, M.S. Takriff (2021) Insights into corrosion inhibition behavior of a 5-mercapto-1,2,4-triazole derivative for mild steel in hydrochloric acid solution: experimental and DFT studies. Lubricants, 9(12), 122, https://doi.org/10.3390/lubricants9120122.

[18] A. Alamiery (2021) Short report of mild steel corrosion in 0.5 M H2SO4 by 4-ethyl-1-(4-oxo-4-phenylbutanoyl) thiosemicarbazide. J. Tribologi, 30, 90–99.

[19] A.A. Alamiery, W.N.R.W. Isahak, M.S. Takriff (2021) Inhibition of mild steel corrosion by 4-benzyl-1-(4-oxo-4-phenylbutanoyl)thiosemicarbazide: gravimetrical, adsorption and theoretical studies. Lubricants, 9(9), 93, https://doi.org/10.3390/lubricants9090093.

[20] M.A. Dawood, Z.M.K. Alasady, M.S. Abdulazeez, D.S. Ahmed, G.M. Sulaiman, A.A.H. Kadhum, L.M. Shaker, A.A. Alamiery (2021) The corrosion inhibition effect of a pyridine derivative for low carbon steel in 1 M HCl medium: complemented with antibacterial studies. Int. J. Corr. Scale Inhib., 10(5), 1766–1782.

[21] A. Alamiery (2021) Corrosion inhibition effect of 2-N-phenylamino-5-(3-phenyl-3-oxo-1-propyl)-1,3,4-oxadiazole on mild steel in 1 M hydrochloric acid medium: insight from gravimetric and DFT investigations. Mater. Sci. Energy Technol., 4, 398–406, https://doi.org/10.1016/j.mset.2021.09.002.

[22] A.A. Alamiery (2021) Anticorrosion effect of thiosemicarbazide derivative on mild steel in 1 M hydrochloric acid and 0.5 M sulfuric acid: gravimetrical and theoretical studies. Mater. Sci. Energy Technol., 4, 263–273, https://doi.org/10.1016/j.mset.2021.07.004.

[23] A.A. Alamiery, W.N.R.W. Isahak, H.S.S. Aljibori, H.A. Al-Asadi, A.A.H. Kadhum (2021) Effect of the structure, immersion time and temperature on the corrosion inhibition of 4-pyrrol-1-yln-(2,5-dimethyl-pyrrol-1-yl)benzoylamine in 1.0 M HCl solution. Int. J. Corr. Scale Inhib., 10(6), 700–713, https://doi.org/10.17675/2305-6894-2021-10-2-14.

[24] A. Alamiery, E. Mahmoudi, T. Allami (2021) Corrosion inhibition of low-carbon steel in hydrochloric acid environment using a Schiff base derived from pyrrole: gravimetric and computational studies. Int. J. Corr. Scale Inhib., 10(4), 749–765.

[25] A.J.M. Eltmimi, A. Alamiery, A.J. Allami, R.M. Yusop, A. Kadhum, T. Allami (2021) Inhibitive effects of a novel efficient Schiff base on mild steel in hydrochloric acid environment. Int. J. Corr. Scale Inhib., 10(3), 634–648.

[26] A.L. Alamiery, L.M. Shaker, T. Allami, A.H. Kadhum, M.S. Takriff (2021) A study of acidic corrosion behavior of furan-derived Schiff base for mild steel in hydrochloric acid environment: Experimental, and surface investigation. Materials Today: Proceedings, 44(6), 2337–2341.

[27] B.S. Mahdi, H.S.S. Aljibori, M. Abbass, W.K. Al-Azzawi, A.H. Kadhum, M.M. Hanoon, W.N.R.W. Isahak, A.A. Al-Amiery, H.Sh. Majdi (2022) Gravimetric analysis and quantum chemical assessment of 4-aminoantipyrine derivatives as corrosion inhibitors. International Journal of Corrosion and Scale Inhibition, 11(9), 1191–1213.

[28] S. Junaedi, A.A. Al-Amiery, A. Kadihum, A.A.H. Kadhum, A.B. Mohamad (2013) Inhibition effects of a synthesized novel 4-aminoantipyrine derivative on the corrosion of mild steel in hydrochloric acid solution together with quantum chemical studies. International Journal of Molecular Sciences, 14(6), 11915–11928, https://doi.org/10.3390/ijms140611915.

[29] S.B. Al-Baghdadi, A.A. Al-Amiery, T.S. Gaaz, A.A.H. Kadhum (2021) Terephthalohydrazide and isophthalohydrazide as new corrosion inhibitors for mild steel in hydrochloric acid: Experimental and theoretical approaches. Koroze a ochrana materiálů, 65(8), 12–22.

[30] S. Al-Baghdadi, T.S. Gaaz, A. Al-Adili, A.A. Al-Amiery, M.S. Takriff (2021) Experimental studies on corrosion inhibition performance of acetylthiophene thiosemicarbazone for mild steel in HCl complemented with DFT investigation. International Journal of Low-Carbon Technologies, 16(6), 181–188, https://doi.org/10.1093/ijlct/ctaa050.

[31] M.S. Abdulazeez, Z.S. Abdullahe, M.A. Dawood, Z.K. Handel, R.I. Mahmood, O. Osamah, A.H. Kadhum, L.M. Shaker, A.A. Al-Amiery (2021) Corrosion inhibition of low carbon steel in HCl medium using a thiadiazole derivative: weight loss, DFT studies and antibacterial studies. Int J Corr Scale Inhib, 10(6), 1812–1828.

[32] A.M. Mustafa, F.F. Sayyid, N. Betti, M.M. Hanoon, A. Al-Amiery, A.A.H. Kadhum, M.S. Takriff (2021) Inhibition evaluation of 5-(4-(1H-pyrrol-1-yl)phenyl)-2-mercapto-1,3,4-oxadiazole for the corrosion of mild steel in an acid environment: thermodynamic and DFT aspects. Tribologia, 38(4), 39-47. https://doi.org/10.30678/FJT.105330

[33] ASTM International, Standard Practice for Preparing, Cleaning, and Evaluating Corrosion Test, 2011, 1–9.

[34] NACE International, Laboratory Corrosion Testing of Metals in Static Chemical Cleaning Solutions at Temperatures below 93°C (200°F), TM0193-2016-SG, 2000.

[35] M.M. Hanoon, A.M. Resen, L.M. Shaker, A.A.H. Kadhum, A.A. Al-Amiery (2021) Corrosion investigation of mild steel in aqueous hydrochloric acid environment using N-(naphthalen-1yl)-1-(4-pyridinyl)methanimine complemented with antibacterial studies. Biointerface Res. Appl Chem, 11(6), 9735–9743.

[36] A.A. Al-Amiery, W.K. Al-Azzawi, W.N.R.W. Isahak (2022) Isatin Schiff base is an effective corrosion inhibitor for mild steel in hydrochloric acid solution: gravimetrical, electrochemical, and computational investigation. Sci Rep, 12(4), 17773. https://doi.org/10.1038/s41598-022-22611-4

[37] A. Al-Amiery, W.N.R.W. Isahak, W.K. Al-Azzawi (2023) Multimethod evaluation of a 2-(1,3,4-thiadiazole-2-yl)pyrrolidine corrosion inhibitor for mild steel in HCl: combining gravimetric, electrochemical, and DFT approaches. Sci Rep, 13(4), 9770. https://doi.org/10.1038/s41598-023-36252-8

[38] A.A. Al-Amiery (2021) Anti-corrosion performance of 2-isonicotinoyl-N-phenylhydrazinecarbothioamide for mild steel hydrochloric acid solution: Insights from experimental measurements and quantum chemical calculations. Surf Rev Lett, 28(3), 2050058. https://doi.org/10.1142/S0218625X20500584

[39] Y.M. Abdulsahib, A.J.M. Eltmimi, S.A. Alhabeeb, M.M. Hanoon, A.A. Al-Amiery, T. Allami, A.A.H. Kadhum (2021) Experimental and theoretical investigations on the inhibition efficiency of N-(2,4-dihydroxytolueneylidene)-4-methylpyridin-2-amine for the corrosion of mild steel in hydrochloric acid. Int J Corr Scale Inhib, 10(6), 885–899.

[40] M.J. Frisch, G.W. Trucks, H.B. Schlegel, G.E. Scuseria, M.A. Robb, J.R. Cheeseman, J.A. Montgomery, T. Vreven, K.N. Kudin, J.C. Burant, J.M. Millam, S.S. Iyengar, J. Tomasi, V. Barone, B. Mennucci, M. Cossi, G. Scalmani, N. Rega, N. Petersson, H. Nakatsuji, H. Hada, M. Ehara, R. Toyota, R. Fukuda, J. Hasegawa, M. Ishida, T. Nakajima, Y. Honda, O. Kitao, H. Nakai, M. Klene, X. Li, J.E. Knox, H.P. Hratchian, J.B. Cross, V. Bakken, C. Adamo, J. Jaramillo, R. Gomperts, R.E. Stratmann, O. Yazyev, A.J. Austin, R. Cammi, C. Pomelli, J.W. Ochterski, J.W. Ayala, P.Y. Morokuma, G.A. Voth, P. Salvador, J.J. Dannenberg, V.G. Zakrzewski, S. Dapprich, A.D. Daniels, M.C. Strain, O. Farkas, D.K. Malick, A.D. Rabuck, K. Raghavachari, J.B. Foresman, J.V. Ortiz, Q. Cui, A.G. Baboul, S. Clifford, J. Cioslowski, B.B. Stefanov, G. Liu, A. Liashenko, P. Piskorz, I. Komaromi, R.L. Martin, R.L. Fox, T. Keith, M.A. Al-Laham, C.Y. Peng, A. Nanayakkara, M. Challacombe, P.M.W. Gill, B. Johnson, W. Chen, M.W. Wong, C. Gonzalez, J.A. Pople (2004) Gaussian 03, Revision B. 05, Gaussian, Inc., Wallingford, CT.

[41] T. Koopmans (1934) Ordering of wave functions and eigenenergies to the individual electrons of an atom. Physica, 1(4), 104–113 (In German).

[42] A.A. Al-Amiery, F. Binti Kassim, A.A.H. Kadhum (2016) Synthesis and characterization of a novel eco-friendly corrosion inhibitor for mild steel in hydrochloric acid. Sci Rep, 6(3), 19890. https://doi.org/10.1038/srep19890

[43] A.K. Khudhair, A.M. Mustafa, M.M. Hanoon, A.A. Al-Amiery, L.M. Shaker, T. Gazz, A.B. Mohamad, A.H. Kadhum, M.S. Takriff (2022) Experimental and theoretical investigation on the corrosion inhibitor potential of N-MEH for mild steel in HCl. Prog Color Colorant Coat, 15(2), 111–122. https://doi.org/10.30509/pccc.2021.166815.1111

[44] D.S. Zinad, R.D. Salim, N. Betti, L.M. Shaker, A.A. Al-Amiery (2022) Comparative investigations of the corrosion inhibition efficiency of a 1-phenyl-2-(1-phenylethylidene)hydrazine and its analog against mild steel corrosion in hydrochloric acid solution. Prog Color Colorant Coat, 15(1), 53–63. https://doi.org/10.30509/pccc.2021.166786.1108

[45] R.D. Salim, N. Betti, M. Hanoon, A.A. Al-Amiery (2021) 2-(2,4-Dimethoxybenzylidene)-N-phenylhydrazinecarbothioamide as an efficient corrosion inhibitor for mild steel in acidic environment. Prog Color Colorant Coat, 15(1), 45–52. https://doi.org/10.30509/pccc.2021.166775.1105

[46] A.A. Al-Amiery, L.M. Shaker, A.H. Kadhum, M.S. Takriff (2021) Exploration of furan derivative for application as corrosion inhibitor for mild steel in hydrochloric acid solution: Effect of immersion time and temperature on efficiency. Mater Today: Proc, 42(6), 2968–2973.

[47] A.M. Resen, M.M. Hanoon, W.K. Alani, A. Kadhim, A.A. Mohammed, T.S. Gaaz, A.A.H. Kadhum, A.A. Al-Amiery, M.S. Takriff (2021) Exploration of 8-piperazine-1-ylmethylumbelliferone for application as a corrosion inhibitor for mild steel in hydrochloric acid solution. Int J Corr Scale Inhib, 10(2), 368–387.

[48] M.M. Hanoon, A.M. Resen, A.A. Al-Amiery, A.A.H. Kadhum, M.S. Takriff (2022) Theoretical and experimental studies on the corrosion inhibition potentials of 2-((6-methyl-2-ketoquinolin-3-yl)methylene) hydrazinecarbothioamide for mild steel in 1 M HCl. Prog Color Colorant Coat, 15(1), 11–23. https://doi.org/10.30509/pccc.2020.166739.1095.

[49] F.G. Hashim, T.A. Salman, S.B. Al-Baghdadi, T. Gaaz, A.A. AlAmiery (2020) Inhibition effect of hydrazine-derived coumarin on a mild steel surface in hydrochloric acid. Tribologia, 37(3), 45–53, https://doi.org/10.30678/FJT.95510.

[50] A.M. Resen, M. Hanoon, R.D. Salim, A.A. Al-Amiery, L.M. Shaker, A.A.H. Kadhum (2020) Gravimetrical, theoretical investigations, and surface morphological investigations of corrosion inhibition effect of 4-(benzoimidazole-2-yl)pyridine on mild steel in hydrochloric acid. Koroze Ochr Mater, 64(1), 122–130, https://doi.org/10.2478/kom-2020-0018.

[51] A.Z. Salman, Q.A. Jawad, K.S. Ridah, L.M. Shaker, A.A. AlAmiery (2020) Selected bisthiadiazole: synthesis and corrosion inhibition studies on mild steel in HCl environment. Surf Rev Lett, 27(3), 2050014.

[52] A.A. Alamiery, W.N.R.W. Isahak, H.S.S. Aljibori, H.A. Al-Asadi, A.A.H. Kadhum (2021) Effect of the structure, immersion time and temperature on the corrosion inhibition of 4-pyrrol-1-yl-N-(2,5-dimethyl-pyrrol-1-yl)benzoylamine in 1.0 M HCl solution. Int J Corr Scale Inhib, 10(5), 700–713.

[53] S.B. Al-Baghdadi, F.G. Hashim, A.Q. Salam, T.K. Abed, T.S. Gaaz, A.A. Al-Amiery, A.A.H. Kadhum, K.S. Reda, W.K. Ahmed (2018) Synthesis and corrosion inhibition application of NATN on mild steel surface in acidic media complemented with DFT studies. Results Phys, 8(6), 1178–1184.

[54] W.K. Al-Azzawi, A.J. Al Adily, F.F. Sayyid, R.K. Al-Azzawi, M.H. Kzar, H.N. Jawoosh, A.A. Al-Amiery, A.A.H. Kadhum, W.N.R.W. Isahak, M.S. Takriff (2022) Evaluation of corrosion inhibition characteristics of an N-propionanilide derivative for mild steel in 1 M HCl: Gravimetrical and computational studies. Int J Corr Scale Inhib, 11(3), 1100–1114.

[55] A.K. Al-Edan, W.N.R.W. Isahak, Z.A.C. Ramli, W.K. Al-Azzawi, A.A.H. Kadhum, H.S. Jabbar, A. Al-Amiery (2023) Palmitic acid-based amide as a corrosion inhibitor for mild steel in 1M HCl. Heliyon, 9(4), e14657, https://doi.org/10.1016/j.heliyon.2023.e14657.

[56] F.F. Sayyid, A.M. Mustafa, M.M. Hanoon, L.M. Saker, A.A. Alamiery (2022) Corrosion protection effectiveness and adsorption performance of schiff base-quinazoline on mild steel in HCl environment. Corros Sci Tech, 21(4), 77–88.

[57] A.A. Al-Amiery, A.B. Mohamad, A.A.H. Kadhum (2022) Experimental and theoretical study on the corrosion inhibition of mild steel by nonanedioic acid derivative in hydrochloric acid solution. Sci Rep, 12(6), 4705, https://doi.org/10.1038/s41598-022-08146-8.

[58] A.A. Al-Amiery, W.N. Isahak, W.K. Al-Azzawi (2024) Sustainable corrosion inhibitors: A key step towards environmentally responsible corrosion control. Ain Shams Engineering Journal, 102672, https://doi.org/10.1016/j.asej.2024.102672.

[59] I. Obot, N. Obi-Egbedi, S. Umoren (2009) Adsorption characteristics and corrosion inhibitive properties of clotrimazole for aluminium corrosion in hydrochloric acid. Int. J. Electrochem. Sci, 4, 863–877.

[60] M.H. Sliem, N.M. El Basiony, E.G. Zaki, M.A. Sharaf, A.M. Abdullah (2020) Corrosion Inhibition of Mild Steel in Sulfuric Acid by a Newly Synthesized Schiff Base: An Electrochemical, DFT, and Monte Carlo Simulation Study. Electroanalysis, 32, 3145–3158, DOI: 10.1002/elan.202060461.

[61] I. Obot, N. Obi-Egbedi, S. Umoren (2009) Antifungal drugs as corrosion inhibitors for aluminium in 0.1 M HCl. Corros. Sci, 51, 1868–1875, doi: 10.1016/j.corsci.2009.05.017.

[62] M. Quraishi, F. Ansari, D. Jamal (2003) Thiourea derivatives as corrosion inhibitors for mild steel in formic acid. Mater. Chem. Phys, 77, 687–690, DOI: 10.1016/S0254-0584(02)00130-X.

[63] J. Fu, H. Zang, Y. Wang, S. Li, T. Chen, X. Liu (2012) Experimental and theoretical study on the inhibition performances of quinoxaline and its derivatives for the corrosion of mild steel in hydrochloric acid. Ind. Eng. Chem. Res, 51, 6377–6386, DOI: 10.1021/ie202832e.

[64] S.K. Saha, P. Ghosh, A. Hens, N.C. Murmu, P. Banerjee (2015) Density functional theory and molecular dynamics simulation study on corrosion inhibition performance of mild steel by mercapto-quinoline Schiff base corrosion inhibitor. Physica E, 66, 332–341, DOI: 10.1016/j.physe.2014.10.035.

[65] A.S. Fouda, M.A. Ismail, A.M. Temraz, A.S. Abousalem (2019) Comprehensive investigations on the action of cationic terthiophene and bithiophene as corrosion inhibitors: experimental and theoretical studies. New J. Chem, 43, 768–789, DOI: 10.1039/C8NJ04330B.

[66] S.K. Saha, P. Banerjee (2018) Introduction of newly synthesized Schiff base molecules as efficient corrosion inhibitors for mild steel in 1 M HCl medium: an experimental, density functional theory and molecular dynamics simulation study. Mater. Chem. Front, 2, 1674–1691, DOI: 10.1039/C8QM00162F.

[67] I. Lukovits, E. Kalman, F. Zucchi (2001) Corrosion inhibitors—correlation between electronic structure and efficiency. Corrosion, 57(1), 3–8.

[68] L. Guo, I.B. Obot, X. Zheng, X. Shen, Y. Qiang, S. Kaya, C. Kaya (2017) Theoretical insight into an empirical rule about organic corrosion inhibitors containing nitrogen, oxygen, and sulfur atoms. Appl. Surf. Sci, 406, 301–306, DOI: 10.1016/j.apsusc.2017.02.134.

[69] M. Masoud, M. Awad, M. Shaker, M. El-Tahawy (2010) The role of structural chemistry in the inhibitive performance of some aminopyrimidines on the corrosion of steel. Corros. Sci, 52, 2387–2396, DOI: 10.1016/j.corsci.2010.04.011.

[70] B.D. Mert, A.O. Yüce, G. Kardaş, B. Yazıcı (2014) Inhibition effect of 2-amino-4-methylpyridine on mild steel corrosion: experimental and theoretical investigation. Corros. Sci, 85, 287–295, DOI: 10.1016/j.corsci.2014.04.032.

[71] N. Labjar, F. Bentiss, M. Lebrini, C. Jama, S. El hajjaji (2011) Study of Temperature Effect on the Corrosion Inhibition of C38 Carbon Steel Using Amino-tris(Methylenephosphonic) Acid in Hydrochloric Acid Solution. Int. J. Corros, 2011, 548528, DOI: 10.1155/2011/548528.

[72] A. Al-Sabagh, N. El Basiony, S. Sadeek, M. Migahed (2018) Scale and corrosion inhibition performance of the newly synthesized anionic surfactant in desalination plants: experimental, and theoretical investigations. Desalination, 437, 45–58, DOI: 10.1016/j.desal.2018.01.036.

[73] E.E. Ebenso, T. Arslan, F. Kandemirli, N. Caner, I. Love (2010) Quantum chemical studies of some rhodanine azosulpha drugs as corrosion inhibitors

for mild steel in acidic medium. Int. J. Quantum Chem, 110, 1003–1018, DOI: 10.1002/qua.22249.
[74] B.G. Bedir, M. Abd El-raouf, S. Abdel-Mawgoud, N.A. Negm, N.M. El Basiony (2021) Corrosion inhibition of carbon steel in hydrochloric acid solution using ethoxylated nonionic surfactants based on schiff base: electrochemical and computational investigations. ACS omega, 6(6), 4300–4312.

IZVOD

ISTRAŽIVANJE FPM-A KAO INHIBITORA KOROZIJE ZA BLAGI ČELIK U RASTVORU HCI: UVIDI IZ ELEKTROHEMIJE, GUBITAK TEŽINE I TEORIJSKI PRISTUPI

U ovoj studiji istražujemo efikasnost furan-2-yl-piperazin-1-yl-metanona (FPM) kao inhibitora korozije za blagi čelik u okruženju HCl. Naša studija kombinuje elektrohemijske tehnike, merenja gubitka težine i proračune teorije funkcionalne gustine (DFT). Što se tiče eksperimenata sa gubitkom težine, otkrili smo da koncentracija od 0,5 mM FPM-a obezbeđuje maksimalnu efikasnost zaštite, dostižući 91,8% na 303 K nakon 30 minuta potapanja i primetili smo da efikasnost inhibicije raste sa povećanjem koncentracije FPM-a, ali opada sa višim temperaturama. Na osnovu Langmuirove izoterme i eksperimentalne analize, može se sugerisati da FPM može da prianja na površinu mekog čelika putem fizičkih i hemijskih interakcija. Štaviše, naše teorijske studije otkrivaju korelacije između strukture FPM-a i njegove efikasnosti u inhibiciji korozije, bacajući svetlo na osnovne mehanizme. I eksperimentalni i teorijski rezultati se slažu.Naši nalazi naglašavaju potencijal FPM-a kao inhibitora korozije u industrijskim primenama, nudeći nove mogućnosti za tehnike kontrole korozije.
Ključne reči: *Furan, korozija, čelik, potenciodinamička polarizacija, DFT*

Naučni rad
Rad primljen: 26.10.2024.
Rad korigovan: 12.12.2024.
Rad prihvacen: 15.12.2024.

Sundus M. Ahmed https://orcid.org/0009-0008-2586-5218
Ali H. Alwazir https://orcid.org/ 0009-0007-9399-142X
Hakim S. Aljibori https://orcid.org/0000-0002-5815-8148
Firas F. Sayyid https://orcid.org/ 0000-0002-6817-335X
Ali M. Mustafa https://orcid.org/ 0000-0002-5226-0926
Ahmed A. Alamiery, https://orcid.org/ 0000-0003-1033-4904
Abdul Amir H. Kadhum https://orcid.org/0000-0003-4074-9123